Energy-dependent collective excitations in Os and Pt isotopes

2017 Phys. Scr. 92 084001

(http://iopscience.iop.org/1402-4896/92/8/084001)

IOP Publishing | Royal Swedish Academy of Sciences Physica Scripta

Phys. Scr. **92** (2017) 084001 (9pp) https://doi.org/10.1088/1402-4896/aa6dab

Energy-dependent collective excitations in Os and Pt isotopes

A I Budaca[1] **and R Budaca**[1,2]

[1] Horia Hulubei National Institute of Physics and Nuclear Engineering, RO-077125 Bucharest-Magurele, Romania
[2] Academy of Romanian Scientists, 54 Splaiul Independentei, Bucharest, RO-050094, Romania

E-mail: rbudaca@theory.nipne.ro

Received 9 February 2017, revised 5 April 2017
Accepted for publication 18 April 2017
Published 12 July 2017

Abstract

An exactly solvable model is constructed by considering an energy-dependent harmonic oscillator potential in the β part of the Bohr Hamiltonian separated adiabatically from the γ-angular degrees of freedom. The energy dependence is linear and introduced in the string constant. The fundamental implications of the energy dependence in quantum theory are thoroughly discussed in connection with the slope parameter. The numerical applications of the model are found to match the collective features for extended chains of even–even Os and Pt isotopes, which exhibit a smooth evolution in the slope of the energy dependence.

Keywords: Bohr Hamiltonian, energy-dependent potential, collective models, Os nuclei, Pt nuclei

(Some figures may appear in colour only in the online journal)

1. Introduction

Exactly solvable models, in particular Schrödinger equations whose solutions can be determined algebraically, play a very important role in quantum physics. Exact solvability is directly related to the symmetry properties of the modeled system. This in turn allows a group theoretical description of the problem in terms of associated quantum numbers. The number of exactly solvable potentials is unfortunately scarce, including the most well-known textbook examples, such as Coulomb, Kratzer, harmonic oscillator, Davidson, Morse, Pöschl–Teller, Scarf, Rosen–Morse, Eckart, Nathanzon and a few others. Many of these potentials were successfully used in various instances of the Bohr–Mottelson model [1, 2] to describe the collective states of even–even atomic nuclei within simple parametric solutions [3, 4]. The diversity of the nuclear collective behavior, however, limits the success of these solutions to particular regions of the nuclide chart, or even only to few nuclei, with many 'exotic' collective excitations unattainable. Nevertheless, some collective models serve as reference landmarks due to their embedded dynamical symmetries [5], thus giving some perspective for the uncharted nuclear collective motion. There are ways to extend the utility of the exactly solvable models. One is their extension to quasi-exact solvability [6], applied, for example, in the case of the sextic potential [7]. Another avenue which will be explored in this paper refers to the energy-dependent variations of the exactly solvable potentials [8–10]. The differential Schrödinger equation with an energy-dependent (non-local) potential is solved similarly to the case of the original local potential, thus retaining at least a part of its analytic structure. The eigenvalues, however, are not determined from a linear correspondence, as in the usual case, but by solving an algebraic equation of higher order [10–15]. This theory was first applied for the Bohr–Mottelson Hamiltonian in connection to the spherical vibrator model where the harmonic potential was made linearly energy-dependent through the string constant [16]. Other applications followed [17, 18], opening up a new class of collective solutions with completely new spectral attributes. In this paper we want to reiterate the formalism of [16] for the axially symmetric nuclei whose Bohr Hamiltonian can be approximately decoupled into two parts corresponding to the shape variables β and γ [19]. Such an adiabatic decoupling provides a theoretical spectrum classified in well-defined rotational bands. This is achieved in the next section where the analytical formulas of the theoretical formalism are deduced. Due to the distinctive structure of the five-dimensional shape

phase space associated with the Bohr Hamiltonian, the implications coming from the energy dependence of the potential will be necessarily revised in section 3. As most of the medium mass nuclei exhibiting collective features are axially deformed, such a description is expected to have a larger applicability than the previous γ-unstable solutions [16, 17]. This is confirmed by the model's numerical applications on an extended series of Os and Pt isotopes presented in section 4. The theoretical fits also revealed some regularities in the energy dependence throughout the isotopic chains which differ between Os and Pt nuclei. This result, as well as other conclusions regarding the present study, are recounted in the final section.

2. Theoretical framework

The general Bohr Hamiltonian reads [1, 2]:

$$H=-\frac{\hbar^2}{2B}\left[\frac{1}{\beta^4}\frac{\partial}{\partial\beta}\beta^4\frac{\partial}{\partial\beta}+\frac{1}{\beta^2\sin 3\gamma}\frac{\partial}{\partial\gamma}\sin 3\gamma\frac{\partial}{\partial\gamma}-\frac{1}{4\beta^2}\sum_{k=1}^{3}\frac{Q_k^2}{\sin^2\left(\gamma-\frac{2}{3}\pi k\right)}\right]+V(\beta,\gamma). \quad (1)$$

whereby $Q_k (k = 1, 2, 3)$ are denoted the operators of the total angular momentum projections on the axes of the intrinsic reference frame, while B is the mass parameter. In the case of a very sharp γ potential centered around $\gamma = 0$, the rotational term from (1) can be very well approximated [19] by

$$\sum_{k=1}^{3}\frac{Q_k^2}{\sin^2\left(\gamma-\frac{2}{3}\pi k\right)}\approx\frac{4}{3}\mathbf{Q}^2+Q_3^2\left(\frac{1}{\sin^2\gamma}-\frac{4}{3}\right), \quad (2)$$

where $\mathbf{Q}$ is the total angular momentum vector operator.

Seeking solutions of the factorized form $\Psi(\beta, \gamma, \Omega) = \xi(\beta)\eta(\gamma)D^L_{MK}(\Omega)$ where D^L_{MK} are Wigner functions of total angular momentum L and its projections M and K on the body-fixed and laboratory-fixed z-axis respectively, the total Schrödinger equation can be resolved after averaging on the Wigner states into β and γ parts [19]:

$$\left[-\frac{1}{\beta^4}\frac{\partial}{\partial\beta}\beta^4\frac{\partial}{\partial\beta}+\frac{L(L+1)}{3\beta^2}+u(\beta)\right]\xi(\beta)=\epsilon^\beta\xi(\beta), \quad (3)$$

$$\left[-\frac{1}{\beta_0^2\sin 3\gamma}\frac{\partial}{\partial\gamma}\sin 3\gamma\frac{\partial}{\partial\gamma}+\frac{K^2}{4\beta_0^2}\left(\frac{1}{\sin^2\gamma}-\frac{4}{3}\right)+v(\gamma)\right]\times\eta(\gamma)=\epsilon^\gamma\eta(\gamma). \quad (4)$$

Here β_0 is a static 'average' of β which ensures an approximated adiabatic separation of the β and γ surface oscillations, provided a similar separation is valid for the potential energy $\frac{2B}{\hbar^2}V(\beta, \gamma) = v(\beta) + v(\gamma)$. This approximation was extensively analysed in [20], and it was concluded that it is in agreement with the full diagonalization results for most of the transitional nuclei. In the context of this adiabatic separation, the total energy of the system is expressed as $\epsilon = \epsilon^\beta + \epsilon^\gamma = \frac{2B}{\hbar^2}E$.

The γ equation is further approximated by a first order expansion of the trigonometric functions around $\gamma = 0$ [19, 20]. Considering the same approximation for the lowest order γ potential $v(\gamma) = a(1 - \cos 3\gamma)$, which obeys the Bohr symmetry [23], one obtains a radial-like equation for a two-dimensional harmonic oscillator

$$\left[-\frac{1}{\beta_0^2\gamma}\frac{\partial}{\partial\gamma}\gamma\frac{\partial}{\partial\gamma}+\left(\frac{K}{2}\right)^2\frac{1}{\beta_0^2\gamma^2}+(3a)^2\frac{\gamma^2}{2}\right]\times\eta(\gamma)=\left(\epsilon^\gamma+\frac{K^2}{3\beta_0^2}\right)\eta(\gamma). \quad (5)$$

The eigensystem for the γ variable is then easily solved and the results are:

$$\epsilon^\gamma_{Kn_\gamma}=\frac{3a}{\beta_0}(n_\gamma+1)-\frac{K^2}{3\beta_0^2},\ n_\gamma=0,1,2,\ldots, \quad (6)$$

$$\eta_{n_\gamma K}(\gamma)=N_{nK}\gamma^{|\frac{K}{2}|}e^{-3a\frac{\gamma^2}{2}}L_n^{|\frac{K}{2}|}(3a\gamma^2), \quad (7)$$

$$n=\frac{n_\gamma-\frac{|K|}{2}}{2},\ K=\begin{cases}0,\pm 2n_\gamma,\ n_\gamma-\text{even}\\ \pm 2n_\gamma,\ n_\gamma-\text{odd}\end{cases} \quad (8)$$

where N_{nK} is a normalization constant determined with the integration measure $|\sin 3\gamma| d\gamma$.

Considering a harmonic oscillator potential for the β equation (3) also, but with a coupling constant depending on the energy associated only with the β degree of freedom $v(\beta, \epsilon^\beta) = k(\epsilon^\beta)\beta^2$, one obtains a similar exact solution:

$$F_{Ln_\beta}(\beta)=N_{Ln_\beta}[k(\epsilon^\beta)]^{\frac{p}{2}}\beta^p e^{-\frac{k(\epsilon^\beta)\beta^2}{2}}\times L_{n_\beta}^{p+\frac{3}{2}}(k(\epsilon^\beta)\beta^2), \quad (9)$$

where N_{Ln_β} is a normalization factor which depends on the chosen energy dependence $k(\epsilon)$, and

$$p=\frac{1}{2}\left[\sqrt{9+\frac{4}{3}L(L+1)}-3\right]. \quad (10)$$

The corresponding energy eigenvalues are then extracted from the following equation:

$$\epsilon^\beta_{Ln_\beta}=\sqrt{k(\epsilon^\beta_{Ln_\beta})}\left(2n_\beta+p+\frac{5}{2}\right). \quad (11)$$

When k is a constant, the model becomes fully scalable with respect to it, thus leading to the $X(5)$-β^2 solution [21] which is parameter free for $K = 0$ states.

Due to the energy dependence of the β potential, the scalar products involving β wave functions (9) are defined with the modified integration measure [10]:

$$\beta^4 d\beta\ \rightarrow\left[1-\frac{\partial v(\beta,\epsilon^\beta)}{\partial\epsilon^\beta}\right]\beta^4 d\beta. \quad (12)$$

This is one of the essential conditions for the corresponding quantum theory to be intrinsically consistent [10], ensuring that the wave functions (9) satisfy the continuity equation. We

will further use the simplest energy dependence, i.e. the linear one

$$k(\epsilon^{\beta}_{Ln_\beta}) = 1 + a\epsilon^{\beta}_{Ln_\beta}. \tag{13}$$

In the general case of an arbitrary energy dependence, the eigenfunctions associated with each energy level correspond to different Hamiltonian operators acting in distinct Hilbert spaces due to the variation of the potential involved. The fact that the resulting wave-functions do not belong to the same eigenspace leads to the violation of the completeness relation. By amending this relation with the same correction factor as in the case of the scalar product, the completeness condition is exactly satisfied only if the correction factor is state independent [10], and this happens only for the linear energy dependence. Other energy dependencies have deviations from the completeness relation, a fact which makes the calculation of expectation values unreliable. Therefore, in the present study, all scalar products involving functions of β must be amended with the same factor $(1 - a\beta^2)$. This is also the case for the norm N_{Ln_β}.

Plugging (13) into (11), we obtain a quadratic equation for the β energy, where the physical solution is

$$\epsilon^{\beta}_{Ln_\beta} = \frac{a}{2}\left(2n_\beta + p + \frac{5}{2}\right)^2 + \left(2n_\beta + p + \frac{5}{2}\right)\sqrt{1 + \frac{a^2}{4}\left(2n_\beta + p + \frac{5}{2}\right)^2}. \tag{14}$$

Finally, the total excitation energy of the system is given as a sum of the γ (6) and β (14) eigenvalues

$$E_{LKn_\beta n_\gamma} = \frac{\hbar^2}{2B}\left[\frac{a}{2}\left(2n_\beta + 1 + \sqrt{\frac{9}{4} + \frac{L(L+1)}{3}}\right)^2 + \left(2n_\beta + 1 + \sqrt{\frac{9}{4} + \frac{L(L+1)}{3}}\right) \times \sqrt{1 + \frac{a^2}{4}\left(2n_\beta + 1 + \sqrt{\frac{9}{4} + \frac{L(L+1)}{3}}\right)^2} - \frac{K^2}{3\beta_0^2} + \frac{3a}{\beta_0}(n_\gamma + 1)\right], \tag{15}$$

while the total wave-function, including the normalized and symmetrized angular part, is [19, 22, 24]:

$$\Psi_{LMKn_\beta n_\gamma}(\beta, \gamma, \Omega) = F_{Ln_\beta}(\beta)\eta_{n_\gamma|K|}(\gamma) \times \sqrt{\frac{2L+1}{16\pi^2(1+\delta_{K,0})}}\,[D^L_{MK}(\Omega) + (-)^L D^L_{M-K}(\Omega)]. \tag{16}$$

Electromagnetic properties of collective states are dominated by the $B(E2)$ transition probabilities. The quadrupole transition operator used for the calculation of the $E2$ transition probabilities is

$$T_\mu(E2) = t\beta\left[D^2_{\mu 0}\cos\gamma + \frac{1}{\sqrt{2}}(D^2_{\mu 2} + D^2_{\mu -2})\sin\gamma\right], \tag{17}$$

where t is a scaling factor. Exploiting the factorized character of the total wave function (16) and the Wigner–Eckart theorem, one can write the transition probability in a similar manner as [24, 25]:

$$\begin{aligned} &B(E2, LKn_\beta n_\gamma \to L'K'n'_\beta n'_\gamma) \\ &= \frac{5}{16\pi}\frac{|\langle\Psi_{L'K'n'_\beta n'_\gamma}||T(E2)||\Psi_{LKn_\beta n_\gamma}\rangle|^2}{2L+1} \\ &= \frac{5t^2}{16\pi}(C^{L\,2\,L'}_{KK'-KK'}B^{Ln_\beta}_{L'n'_\beta}G^{Kn_\gamma}_{K'n'_\gamma})^2, \end{aligned} \tag{18}$$

where C is a Clebsch–Gordan coefficient, while factors B and G are integrals over β and γ variables, respectively. In our model γ is very small such that $\cos\gamma \approx 1$ and $\sin\gamma \approx 0$ [24], consequently $G \approx 1$ for $\Delta K = 0$ transitions which are of more interest. One must also remember here the use of the modified integration measure (12) for the β integral.

3. Model characteristics

The energy dependence of the potential has important effects on the quantum structure of the usual state independent problem. The mentioned deformation of the integration metric defining the scalar products of the β shape variable also induces a modification of the associated density of the probability distribution,

$$\rho_{Ln_\beta}(\beta) = |F_{Ln_\beta}(\beta)|^2(1 - a\beta^2)\beta^4. \tag{19}$$

This quantity must be positive definite in order to describe a coherent quantum model. This condition is exactly realized for the whole domain of the β values only when $a \leqslant 0$. Even so, all norms and relevant averages of the β shape variable are positive for any a, L and n_β. Indeed, by taking into consideration expression (14) of the β energy, it can be easily verified, for example, that the norm

$$(N_{Ln_\beta})^{-2} = \frac{\left(n_\beta + p + \frac{3}{2}\right)!}{2(1 + a\epsilon^{\beta}_{Ln_\beta})^{5/2}n_\beta!} \times \left[1 - \frac{a}{1 + a\epsilon^{\beta}_{Ln_\beta}}\left(2n_\beta + p + \frac{5}{2}\right)\right], \tag{20}$$

is positive for $\forall L, n_\beta$ when $a > 0$. Compared to the $a = 0$ situation, the redefined norm for the ground state has an increasing value with the slope parameter. Regardless of the a value, the norm reaches very low values at the same high angular momentum L for a fixed n_β. A more drastic change happens in its evolution with the β vibration quantum number. For $L = 0$, the norm is an asymptotically decreasing

function of n_β when $a = 0$, but at some value of $a > 0$ it starts to increase with n_β. This transition happens at a relatively low value of a, around 0.2, where it also exhibits a local minimum for $n_\beta > 0$.

The notion of negative probability dates from the foundation of quantum mechanics, when Dirac [26] and Heisenberg [27] were first confronted with the case of probability distributions with negative values. They argued that negative probabilities are indispensable when dealing with quantum corrections. The most familiar example in this sense is the Wigner quasi-probability function [28] which associates a phase space probability distribution with the solutions of the Schrödinger equation. The occurrence of negative probability in quantum theory stems from the fact that the quantum hypotheses and initial conditions are not directly transferable to the real physical world. Feynman's conclusion comes to mind here [29]: '*...that a situation for which a negative probability is calculated is impossible, not in the sense that the chance for it happening is zero, but rather in the sense that the assumed conditions of preparation or verification are experimentally unattainable.*' Although the interpretation of negative probability is still a controversial matter, it is nevertheless regarded as a solid mathematical concept [30] which is allowed in quantum theory when dealing with intermediate quantities, i.e. not finally observed [29]. This is also the situation of the probability distribution (19), which is not directly observed because one cannot perform identical measurements to determine the frequency of the appearance for a certain β deformation. It provides, however, physically meaning observables such as expectation values.

For the present case, however, the negative contribution to the total probability distribution is easily negligible for any $a > 0$. Indeed, the maximum negative contribution of ρ amounts to 0.71%, 0.40% and 0.24% for $a = 0.45$, 0.39 and 0.25 from the norms corresponding to $(L, n_\beta) = (0, 0), (2, 0), (0, 1)$ states. The percentage decreases even more with an increase in a and any of the quantum numbers L or n, tending to zero in their asymptotic limits [16]. From a phenomenological point of view, the $a > 0$ and $a < 0$ model realizations correspond to a stiffening and, respectively, a softening of the β vibrations.

Another peculiar feature of the models involving potentials with coupling constants linear in energy is the saturation of the relative energy level spacings in the large value limit of a [16, 17]. The same saturation of the normalized $K = 0$ energy spectrum of the present model can be observed in figure 1. It occurs as a consequence of a becoming a simple scaling factor for the β energy when it reaches a sufficiently high value,

$$\lim_{a\to\infty} \epsilon^{\beta}_{Ln_\beta} = a\left[2n_\beta + 1 + \sqrt{\frac{9}{4} + \frac{L(L+1)}{3}}\right]^2. \qquad (21)$$

One can see from figure 1 that the scaled spectrum can be achieved already at quite moderate values of a for the lowest energy levels. The energy level spectrum of the ground and β bands in the asymptotic limit of a is visualized in figure 2. The associated quadrupole transition rates, shown in the same figure,

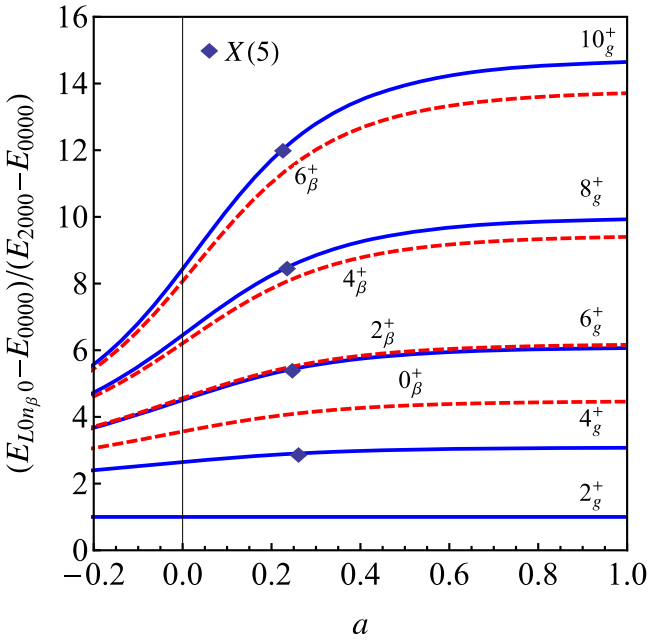

Figure 1. The low-lying excitation energy spectrum of the ground band and the first β excited band ($n_\beta = 1$) normalized to the energy of the first excited state from the ground band are given as a function of the slope parameter a. The points of the intersection between $X(5)$ and the present model estimations of the ground band energy levels are indicated by diamonds.

are calculated numerically with equation (18) by gradually increasing the slope parameter a until a convergence is achieved [16]. Among specific signatures of this asymptotic regime, one can mention the extremely strong $0^+_\beta \to 2^+_g$ transition and the decreasing trend of the intraband transitions starting from $4^+ \to 2^+$. As can be seen from figure 3, this last aspect is very different from the unperturbed case of the $X(5)$-β^2 model, whose ground band to ground band transition probabilities increase linearly. This means that the transition probabilities are more sensible to the variation of a than the energy levels, and that the present model can cover a very wide range of evolution patterns for the transition rates.

The region of negative values for a presents little practical importance. The collective excitations are usually associated with the ratio between the excitation energies of the first two excited states $R_{4/2} > 2$. Although the model recovers the limiting value $R_{4/2} = 2$ for $a = -0.78$, the associated level scheme has monotonically decreasing consecutive level spacings which end in an energy threshold. Such a situation is found, for example, in the ground band of $^{200-218}$Po isotopes [31–33], but is ascribed to a close interplay between single-particle and collective degrees of freedom. To date, pure collective behavior with such a spectrum has not been indicated in any nuclei. Nevertheless, small negative values of a can still ensure an expanding energy level sequence up to high angular momentum states, a fact which further extends the applicability of the proposed model for the description of collective spectra.

From figure 1, one can also see that the ground band energy level sequence of $X(5)$ [19] is very closely reproduced by the present model for $a \sim 0.23$. The β band states are,

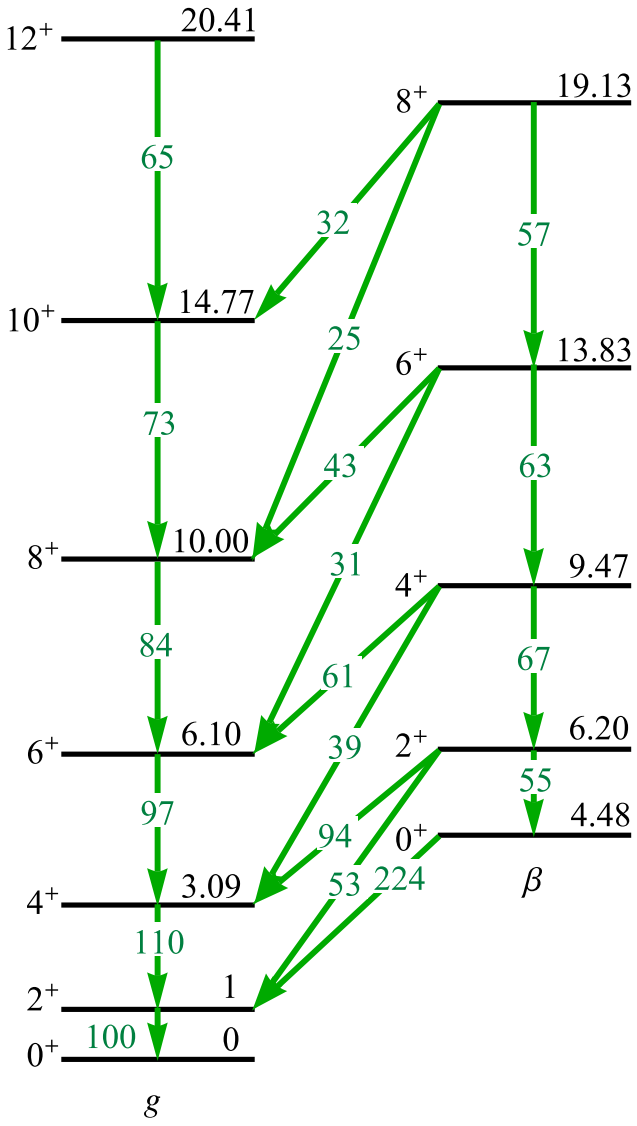

Figure 2. Energy level scheme of the ground band and the first β excited band corresponding to the asymptotic regime of the slope parameter a associated with the energy-dependent $X(5)$-β^2 model. Energies are given in terms of the first excited state energy, while the corresponding $B(E2)$ transition probabilities are normalized to $B(E2, 2_g^+ \to 0_g^+) = 100$ in order to lose the corresponding scaling constants.

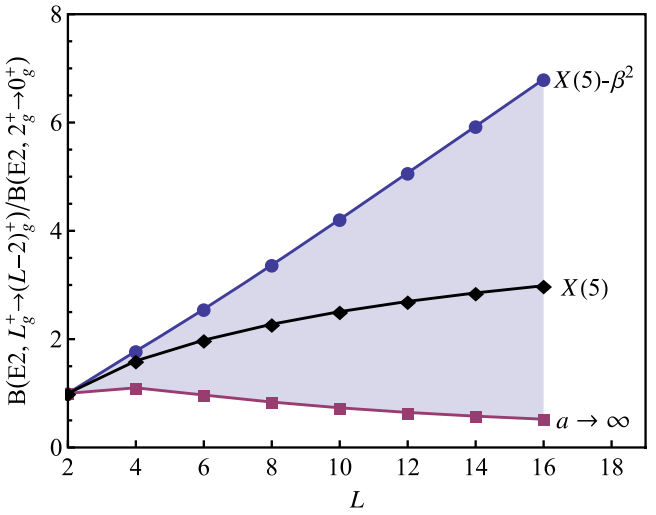

Figure 3. The evolution of the $B(E2)$ transition probabilities within the ground band normalized to $B(E2, 2_g^+ \to 0_g^+)$ as a function of angular momentum for $a = 0$ ($X(5)$-β^2) and $a \to \infty$ which enclose the existence region of the model (gray area). The curve corresponding to the $X(5)$ results is also shown for reference.

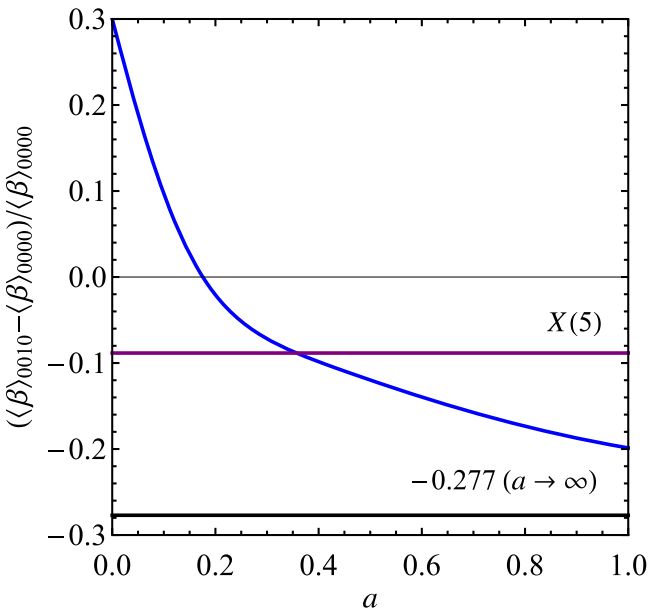

Figure 4. The relative displacement of the average β deformation in the $n_\beta = 1$ state from the ground state value.

however, lower in energy than in the $X(5)$ model. Being based on the *a priori* delocalization of the β deformation, $X(5)$ has an equilibrium value of β vibration smaller than in the ground state. On the other hand, a confined β potential of the harmonic type used in the $X(5)$-β^2 solution leads to a very large increase of the β vibrational equilibrium value. The present approach allows a transition between such situations, i.e. from an expansion to a contraction of the equilibrium β deformation within a vibrational regime relative to the ground state deformation. This transition is graphically shown in figure 4 as a function of a. At $a = 0.176$, the average β deformation in the ground state is equal to that calculated in the first excited β state.

4. Numerical results

The search for experimental realizations of the model was made by minimizing the deviation:

$$\sigma = \sqrt{\frac{1}{N-1}\sum_{i=1}^{N}\left[\frac{E_i(\mathrm{Th})}{E_{2_g^+}(\mathrm{Th})} - \frac{E_i(\mathrm{Exp})}{E_{2_g^+}(\mathrm{Exp})}\right]^2}, \qquad (22)$$

against the variation of the free parameters represented here by slope a and the γ band energy shift

$$D = \frac{3a}{\beta_0} - \frac{4}{3\beta_0^2}. \qquad (23)$$

Table 1. Comparison of theoretical results with the experimental data for the $R_{4/2}$ ratio and the excited band heads. The origin of experimental data is given in the second column. The details of the fitting procedure are the values of the free parameters, the angular momenta of the highest levels of the ground, β, and γ bands included in the fit, as well as the states with missing data denoted by barred values, the total number of the fitted energy levels and the corresponding σ value.

Nucl.	References	$R_{4/2}$ exp	$R_{4/2}$ th	$R_{2/2}$ exp	$R_{2/2}$ th	$R_{0/2}$ exp	$R_{0/2}$ th	a	D	L_g	L_γ	L_β	Nr. of states	σ
^{172}Os	[56]	2.66	2.70	4.03	4.25	3.33	3.67	0.0416	2.045	22	6	8	20	0.79
^{174}Os	[57]	2.74	2.76	5.34	5.92	3.44	3.80	0.0967	3.580	32	5	6/2	22	0.36
^{176}Os	[58, 59]	2.93	2.83	6.39	6.99	4.45	3.95	0.1661	5.181	24	5	6	19	0.73
^{178}Os	[60]	3.01	2.85	6.54	7.57	4.93	4.00	0.1926	6.055	24	7/6	6	20	0.89
^{180}Os	[61]	3.09	2.92	6.59	7.52	5.57	4.15	0.2887	7.430	14	9/8	6	17	0.75
^{190}Os	[62]	2.82	2.93	2.38	3.19	4.65	4.17	0.3032	2.571	10	10/7, 9	2	13	0.24
^{192}Os	[63]	2.82	2.87	2.38	2.69	4.65	4.03	0.2133	1.632	12	10/9	2	15	0.27
^{180}Pt	[61]	2.68	2.80	4.42	5.44	3.12	3.89	0.1360	3.571	26	9/6, 8	6	22	0.56
^{182}Pt	[64]	2.71	2.78	4.31	5.21	3.23	3.84	0.1147	3.209	26	7	8	23	0.70
^{184}Pt	[65]	2.68	2.75	3.98	4.89	3.02	3.78	0.0895	2.780	28	7	6	23	0.52
^{186}Pt	[66]	2.56	2.73	3.17	4.10	2.46	3.74	0.0706	2.110	26	10	6	25	0.58
^{188}Pt	[67]	2.53	2.69	2.28	2.50	3.01	3.66	0.0387	0.938	12	8/5, 7	2	12	0.28
^{190}Pt	[62]	2.49	2.65	2.02	2.23	3.11	3.57	0.0042	0.700	10	6	2	11	0.18
^{192}Pt	[63]	2.48	2.66	1.94	2.20	3.78	3.59	0.0096	0.694	10	8	4	14	0.19
^{194}Pt	[68]	2.47	2.65	1.89	2.01	3.86	3.56	−0.0002	0.564	10	5	6	11	0.19
^{196}Pt	[69, 70]	2.47	2.64	1.94	2.07	3.19	3.55	−0.0049	0.595	10	8	4	13	0.26

N is the total number of the states considered for the fitting procedure. Equation (22) involves excitation energies relative to the ground state, that is the theoretical results are obtained from equation (15) with a subtracted E_{0000} energy. The normalization of these energies to the energy of the first excited state eliminates the dependence on the scaling factor $\hbar^2/2B$. In this way, the energy spectrum of the ground and β bands depends solely on a, D being employed only for the γ band energies.

The best agreement with the experiment was found in an extended series of Os and Pt isotopes. Among these nuclei, ^{174}Os was previously indicated as a viable $X(5)$-β^2 candidate [34]. The results of the fits are given in table 1. The fitted values of the slope parameter a do not exceed unity, with the highest value $a = 0.3032$ reported for ^{190}Os. Therefore, it seems that the asymptotic version of the present model (figure 1) does not have an experimental counterpart in this region of the nuclide chart. There are also two negative a values corresponding to the ^{194,196}Pt nuclei. Although the negative values are quite small and bring only a slight variation to the $X(5)$-β^2 results for the observables listed in table 1, the effect is more significant for higher energy levels, as can be seen from figure 1. The evolution of the slope parameter as a function of the atomic mass number A in each isotopic chain is very smooth and monotonic. There is, however, a stark difference between the two isotopic series: whereas in Os nuclei, a increases with A, for Pt isotopes it has an opposite evolution. A similar reversed behavior was obtained for Os and Pt nuclei with respect to γ-rigidity [39]. It actually originates from the variation of the valence proton–neutron interaction between neutron closed shells at $N = 82$ and $N = 126$ magic numbers. A good measure for this collectivity characteristic is the product between the numbers of valence protons and neutrons [40]. The smaller number of valence nucleons (or holes) in the nuclei near the closed shells allows a softening of the spherical shape of the core against quadrupole vibrations, while a larger valence space facilitates the development of more stable quadrupole deformations [41]. The latter situation is obviously expected near the midshells where the number of valence nucleons is maximal. In Os and Pt isotopes, the relevant neutron midshell is at $N = 104$ corresponding to ^{180}Os and ^{182}Pt. As was discussed alongside the results of figure 4, an increased slope parameter means a more stable deformation, hence the difference between the evolution of the slope parameter in the two isotopic chains. More precisely, the amount of valence proton–neutron interactions in Os nuclei increases up to ^{180}Os and starts to abate afterwards. The latter trend is reflected in the higher a value for ^{190}Os with respect to ^{192}Os and in the general evolution of a for the Pt isotopic chain. Almost all Pt nuclei are positioned above the $N = 104$ midshell, such that their neutron valence spaces are composed from a decreasing number of neutron holes.

Os and Pt isotopes are well known for their ambiguous collective behavior. This fact has made them perfect candidates for many and various collective solutions: γ-rigid [7, 35–39], γ-soft [24, 42–49], or triaxial [7, 36, 37, 50–52]. Moreover, the same region also exhibits features of critical point behavior for the shape phase transition between spherical and deformed nuclei [35–39, 45–47, 53]. This versatility of Os and Pt isotopes is consistent with their central position in the IBA symmetry triangle [54, 55]. Comparing the present results to those of the aforementioned models, one can say that, to date, our model provides the best agreement with experimental energy spectra for all treated nuclei. This statement is based on the comparison of the current description to models with the same or greater number of free

Table 2. Theoretical predictions (first row) for few $\Delta K = 0$ quadrupole transition probabilities are compared with available experimental data (second row). The results are given in W.u. Prediction errors originate from the uncertainty of the experimental $B(E2, 2_g^+ \rightarrow 0_g^+)$ value which is used to determine the scaling factor t.

Nucl. References	$4_g^+ \rightarrow 2_g^+$	$6_g^+ \rightarrow 4_g^+$	$8_g^+ \rightarrow 6_g^+$	$10_g^+ \rightarrow 8_g^+$	$12_g^+ \rightarrow 10_g^+$	$0_\beta^+ \rightarrow 2_g^+$
^{172}Os	200(12)	277(17)	351(21)	419(26)	482(29)	129(8)
[56]	173(17)	300(40)	380(110)	260(50)	280^{+105}_{-45}	
^{174}Os	266(12)	351(16)	421(19)	477(21)	520(23)	158(7)
[57, 71]						
^{176}Os	236(8)	296(10)	337(12)	362(13)	375(13)	138(5)
[72]	243(5)	305(11)	321^{+15}_{-14}	441^{+88}_{-63}	517^{+336}_{-146}	
^{178}Os	225(18)	278(22)	311(25)	328(26)	334(26)	134(11)
[53]			310(230)	340(120)	310(80)	
^{180}Os	221(23)	259(28)	274(29)	274(29)	266(28)	157(17)
[61]	192(25)	160(40)	63(13)			
^{190}Os	112(3)	130(4)	137(4)	136(4)	132(4)	83(2)
[62]	105(6)	113(10)	137(20)	61(16)		2.2(5)
^{192}Os	100(1)	122(1)	134(2)	140(2)	141(2)	61(1)
[63]	75.6(20)	100^{+5}_{-3}	115(6)	105^{+10}_{-26}		0.57(12)
^{180}Pt	256(25)	327(32)	381(37)	418(41)	442(43)	148(14)
[61, 73]	193(16)	198(39)	263(88)			
^{182}Pt	181(13)	248(17)	294(21)	328(23)	353(25)	112(8)
[64]	192(12)	292(20)	266(25)	280(40)	162(10)	
^{184}Pt	215(8)	286(11)	346(14)	395(16)	433(17)	129(5)
[65]	210(8)	226(12)	271(18)	310(40)	183(17)	
^{186}Pt	192(17)	259(23)	319(28)	370(33)	413(37)	118(11)
[74]	181(13)	278(23)	290(30)	291(25)	250(30)	
^{188}Pt	143(26)	198(36)	252(46)	302(55)	348(64)	92(17)
[67]						
^{190}Pt	99(5)	142(8)	187(10)	233(12)	278(15)	68(4)
[62]						
^{192}Pt	101(2)	144(3)	188(4)	233(5)	277(6)	68(1)
[63]	89(5)	70(30)				
^{194}Pt	88(1)	126(2)	166(3)	207(3)	250(4)	60(1)
[68]	85(5)	67(21)	50(14)	34(9)		0.63(14)
^{196}Pt	72.4(4)	104(1)	138(1)	174(1)	210(1)	50.0(2)
[69]	60.0(9)	73^{+4}_{-73}	78^{+10}_{-78}			2.8(15)

parameters. In the case of single parameter solutions, the comparison is restricted only to the ground and β bands which are also specified in the present approach by a single adjustable parameter.

For all considered nuclei, we calculated the absolute values for few $\Delta K = 0$ $E2$ transition probabilities by means of equation (18). We chose to present the results in Weisskopf units (W.u.) for ready use in experimental studies. To obtain absolute values, we fixed the scaling constant t such that to reproduce the experimental value of $B(E2, 2_g^+ \rightarrow 0_g^+)$. The model predictions for the ground band to ground band $E2$ transition rates given in table 2 are in agreement with experimental data for most of the nuclei, especially for transitions involving lower angular momentum states. From all the experimental data for the intraband transitions, only those of ^{176}Os seem to follow the steep increase predicted by the $X(5)$-β^2 model (see figure 3). On the other hand, for the ^{178,190,192}Os nuclei exhibiting the highest values of the slope parameter, the present model predicts the correct stagnation or even decrease in $B(E2)$ values as a function of angular momentum. Although the present numerical applications of the model on the energy spectra are limited to the highest value of $a \approx 0.3$, for some nuclei, the decreasing experimental transition probabilities with angular momentum in the ground band might be better described by a much higher a value. In this way, the gray area from figure 3 representing the existence region of the theoretical model can be fully populated by experimental realizations. The last column of table 2 shows the results of the interband $B(E2, 0_\beta^+ \rightarrow 2_g^+)$ transition rate, which is the most experimentally accessible. The theoretical predictions for this transition overestimate the experimental values by up to two orders of magnitude. One source for this discrepancy is the fact that one used, for this interband transition, a scaling factor fixed from experimental data on an intraband transition. On the other hand, despite good fitting results for nuclei with a measured $0_\beta^+ \rightarrow 2_g^+$ transition, the relative position of the experimental 0_β^+ energy level is not very well reproduced. The energy fits, however, reproduce a correct energy level distribution within the band. Therefore, for more reliable predictions for interband

transitions, one must normalize the results to another transition of the same kind or one connecting two β band states which are yet to be measured. To support this point, one can take as an example the ^{196}Pt nucleus for which more electromagnetic information is available regarding the β band. In this case, the ratio between experimental $2^+_\beta \rightarrow 0^+_\beta$ and $0^+_\beta \rightarrow 2^+_g$ transition probabilities is 1.79(96), while the corresponding theoretical value is 1.29.

5. Conclusions

The Bohr Hamiltonian for axially symmetric nuclei was approximately separated into γ and β parts. The differential equation of the β part includes the rotational contribution from the angular momentum quantum number, while that associated with the γ degree of freedom incorporates the dependence on the angular momentum projection K on the z-axis of the laboratory frame of reference. The γ equation is treated in conformity with the small angle approximation specific to axially symmetric solutions. In this way, the contribution of the γ degree of freedom to the total energy is constant, with an additional shift in the case of the γ band energies. The potential for the rotation–vibration β equation is considered to be of the harmonic oscillator type. The novel ingredient of the present approach is the energy dependence of the potential's coupling constant, which is linear. This modification has important consequences on the fundamental quantum structure of the model which are discussed in detail. The eigenvalue problem for the β part of the Bohr Hamiltonian leads, in this case, to a quadratic equation for the β energy. Apart from a scaling factor, the physical solution depends only on the slope parameter. This means that the ground and β band energies are fully described by a single parameter, while for the γ band energy levels, an additional parameter is needed to fix the band head energy. In its asymptotic limit, the slope parameter acquires just a scaling role, such that the associated β eigensystem becomes parameter independent. The quadrupole transition probabilities are found to be more sensible to the variation of the slope parameter than the energy levels. This is the result of the cumulated energy dependence of the wave functions and the additional a dependence of the integration measure for the β variable scalar product.

The phenomenology associated with an energy-dependent harmonic potential is understood as a stiffening of the nuclear surface against axially-symmetric vibrations. This effect diminishes the displacement of the equilibrium deformation of the β vibration from the ground state deformation. In the zero slope $X(5)$-β^2 model, the β vibrational average deformation is higher than the ground state deformation. As the slope of energy dependence increases, the β vibration equilibrium deformation decreases, becoming at some point even smaller than the ground state value.

The model's numerical applications to many Os and Pt isotopes, whose description in terms of collective solutions has been problematic so far, were found to be in excellent agreement with the experiment concerning the energy spectra as well as quadrupole transition probabilities. The fitted values of the slope parameter have a smooth growth as a function of A in Os isotopes, not reaching, however, into the asymptotic regime. In contrast, the Pt nuclei exhibit a monotonic decrease in the slope of the energy dependence when going to heavier nuclei. This distinctive feature of the Os and Pt isotopic chains shows the importance of excited energy levels in determining their correct collective evolution. The unmatched agreement with the experimental data strongly supports a clear axially-deformed shape for all considered nuclei. This is an encouraging result for future mean field microscopic calculations on excited states. Otherwise, based on the deduced ground state properties of these nuclei, which point to the possible importance of dynamical triaxiality [75–79], their extension to excited states will be hindered by the subsequent restoring of the rotational symmetry [79].

Acknowledgments

This work was supported by the Romanian Ministry of Education and Research, through the project PN-16-42-01-01/2016.

References

[1] Bohr A 1952 *Mat. Fys. Medd. K. Dan. Vidensk. Selsk.* **26** No. 14
[2] Bohr A and Mottelson B 1953 *Mat. Fys. Medd. K. Dan. Vidensk. Selsk.* **27** No. 16
[3] Fortunato L 2005 *Eur. Phys. J.* A **26** 1
[4] Buganu P and Fortunato L 2016 *J. Phys. G: Nucl. Part. Phys.* **43** 093003
[5] Cejnar P, Jolie J and Casten R F 2010 *Rev. Mod. Phys.* **82** 2155
[6] Ushveridze A G 1994 *Quasi-Exactly Solvable Models in Quantum Mechanics* (Bristol: Institute of Physics Publishing)
[7] Budaca R, Buganu P, Chabab M, Lahbas A and Oulne M 2016 *Ann. Phys., NY* **375** 65
[8] Lepage G P 1977 *Phys. Rev.* A **16** 863
[9] Sazdjian H 1988 *J. Math. Phys.* **29** 1620
[10] Formanek J, Lombard R J and Mares J 2004 *Czech. J. Phys.* **54** 289
[11] Lombard R J, Mares J and Volpe C 2007 *J. Phys. G: Nucl. Part. Phys.* **34** 1879
[12] Lombard R J and Mares J 2009 *Phys. Lett.* A **373** 426
[13] Yekken R and Lombard R J 2010 *J. Phys. A: Math. Theor.* **43** 125301
[14] Garcia-Martinez J, Garcia-Ravelo J, Pena J J and Schulze-Halberg A 2009 *Phys. Lett.* A **373** 3619
[15] Yekken R, Lassaut M and Lombard R J 2013 *Few-Body Syst.* **54** 2113
[16] Budaca R 2015 *Phys. Lett.* B **751** 39
[17] Budaca R 2016 *Eur. Phys. J.* A **52** 314
[18] Alimohammadi M and Hassanabadi H 2016 *Int. J. Mod. Phys.* E **25** 1650087
[19] Iachello F 2001 *Phys. Rev. Lett.* **87** 052502
[20] Caprio M A 2005 *Phys. Rev.* C **72** 054323
[21] Bonatsos D, Lenis D, Minkov N, Raychev P P and Terziev P A 2004 *Phys. Rev.* C **69** 014302
[22] Bonatsos D, Lenis D, McCutchan E A, Petrellis D and Yigitoglu I 2007 *Phys. Lett.* B **649** 394

[23] Bohr A and Mottelson B R 1998 *Nuclear Structure* vol 2 (Singapore: World Scientific)
[24] Bonatsos D *et al* 2007 *Phys. Rev.* C **76** 064312
[25] Bijker R, Casten R F, Zamfir N V and McCutchan E A 2003 *Phys. Rev.* C **68** 064304
[26] Dirac P A M 1930 *Proc. Cambridge Philos. Soc.* **26** 376
[27] Heisenberg W 1931 *Physik. Z.* **32** 737
[28] Wigner E P 1932 *Phys. Rev.* **40** 749
[29] Feynman R P 1987 *Negative Probability in Quantum Implications: Essays in Honour of David Bohm* (London: Routledge and Kegan Paul) 235–48
[30] Mückenheim W *et al* 1986 *Phys. Rep.* **133** 337
[31] Yao J M, Bender M and Heenen P-H 2013 *Phys. Rev.* C **87** 034322
[32] Garcia-Ramos J E and Heyde K 2015 *Phys. Rev.* C **92** 034309
[33] Kesteloot N *et al* 2015 *Phys. Rev.* C **92** 054301
[34] Casten R F 2006 *Nat. Phys.* **2** 811
[35] Bonatsos D, Lenis D, Petrellis D, Terziev P A and Yigitoglu I 2006 *Phys. Lett.* B **632** 238
[36] Buganu P and Budaca R 2015 *Phys. Rev.* C **91** 014306
[37] Buganu P and Budaca R 2015 *J. Phys. G: Nucl. Part. Phys.* **42** 105106
[38] Budaca R and Budaca A I 2016 *Phys. Lett.* B **759** 349
[39] Budaca R and Budaca A I 2016 *Phys. Rev.* C **94** 054306
[40] Casten R F 1985 *Phys. Lett.* B **152** 145
[41] Casten R F and Cakirli R B 2016 *Phys. Scr.* **91** 033004
[42] Boztosun I, Bonatsos D and Inci I 2008 *Phys. Rev.* C **77** 044302
[43] Bonatsos D, Georgoudis P E, Lenis D, Minkov N and Quesne C 2011 *Phys. Rev.* C **83** 044321
[44] Bonatsos D, Georgoudis P E, Minkov N, Petrellis D and Quesne C 2013 *Phys. Rev.* C **88** 034316
[45] Raduta A A and Buganu P 2013 *J. Phys. G: Nucl. Part. Phys.* **40** 025108
[46] Raduta A A and Buganu P 2013 *Phys. Rev.* C **88** 064328
[47] Buganu P and Raduta A A 2015 *Rom. J. Phys.* **60** 161
[48] Chabab M, Lahbas A and Oulne M 2015 *Int. J. Mod. Phys.* E **24** 1550089
[49] Çapak M, Petrellis D, Gönül B and Bonatsos D 2015 *Phys G: Nucl. Part. Phys.* **42** 095102
[50] Fortunato L, De Baerdemacker S and Heyde K 2006 *Phys. Rev.* C **74** 014310
[51] Raduta A A and Buganu P 2011 *Phys. Rev.* C **83** 034313
[52] Chabab M, Lahbas A and Oulne M 2015 *Eur. Phys. J.* A **51** 131
[53] Dewald A *et al* 2005 *J. Phys. G: Nucl. Part. Phys.* **31** S1427
[54] McCutchan E A and Zamfir N V 2005 *Phys. Rev.* C **71** 054306
[55] McCutchan E A, Casten R F and Zamfir N V 2005 *Phys. Rev.* C **71** 061301 (R)
[56] Singh B 1995 *Nucl. Data Sheets* **75** 199
[57] Browne E and Junde H 1999 *Nucl. Data Sheets* **87** 15
[58] Basunia M S 2006 *Nucl. Data Sheets* **107** 791
[59] Hao X *et al* 2011 *J. Phys. G: Nucl. Part. Phys.* **38** 025102
[60] Kumar R *et al* 2009 *Phys. Rev.* C **80** 054319
[61] McCutchan E A 2015 *Nucl. Data Sheets* **126** 151
[62] Singh B 2003 *Nucl. Data Sheets* **99** 275
[63] Baglin C M 2012 *Nucl. Data Sheets* **113** 1871
[64] Singh B 2015 *Nucl. Data Sheets* **130** 21
[65] Baglin C M 2010 *Nucl. Data Sheets* **111** 275
[66] Baglin C M 2003 *Nucl. Data Sheets* **99** 1
[67] Singh B 2002 *Nucl. Data Sheets* **95** 387
[68] Singh B 2006 *Nucl. Data Sheets* **107** 1531
[69] Huang X 2007 *Nucl. Data Sheets* **108** 1093
[70] Wahid S G *et al* 2015 *Phys. Rev.* C **92** 054323
[71] Li C B *et al* 2012 *Phys. Rev.* C **86** 057303
[72] Melon B 2011 *PhD Thesis* Universität zu Köln http://kups.ub.uni-koeln.de/4370/ (Accessed: 28 April 2017)
[73] Chen Q M *et al* 2016 *Phys. Rev.* C **93** 044310
[74] Walpe J C *et al* 2012 *Phys. Rev.* C **85** 057302
[75] Sarriguren P, Rodríguez-Guzmán R and Robledo L M 2008 *Phys. Rev.* C **77** 064322
[76] Robledo L M, Rodríguez-Guzmán R and Sarriguren P 2009 *J. Phys. G: Nucl. Part. Phys.* **36** 115104
[77] Nomura K, Otsuka T, Rodríguez-Guzmán R, Robledo L M and Sarriguren P 2011 *Phys. Rev.* C **84** 054316
[78] Garcia-Ramos J E, Heyde K, Robledo L M and Rodríguez-Guzmán R 2014 *Phys. Rev.* C **89** 034313
[79] Rodríguez-Guzmán R, Sarriguren P, Robledo L M and García-Ramos J E 2010 *Phys. Rev.* C **81** 024310